ELSEVIER

Journal of Power Sources 62 (1996) 107–112

JOURNAL OF POWER SOURCES

Characterization and electrochemical properties of $C_x(VOF_3)F$ as positive material for primary lithium batteries

H. Groult [a,*], T. Nakajima [b], N. Kumagai [c], D. Devilliers [a]

[a] Université Pierre et Marie Curie, Laboratoire d'Electrochimie, CNRS URA 430, 4 place Jussieu, 75252 Paris Cedex 05, France

[b] Division of Polymer Chemistry, Graduate School of Engineering, Kyoto University, Sakyo-ku, Kyoto 606-01, Japan

[c] Department of Applied Chemistry, Faculty of Engineering, Iwate University, Ueda 4-3-5, Morioka 020, Japan

Received 17 January 1996; revised 19 February 1996; accepted 19 March 1996

Abstract

Vanadium oxide fluoride–graphite intercalation compounds, i.e. $C_x(VOF_3)F$ with $17.2 \leq x \leq 38.8$, have been prepared from V_2O_5 and graphite in a fluorine atmosphere at 130 °C. The structural characteristics of these compounds have been deduced from X-ray diffraction and X-ray photoelectron spectroscopy measurements. Intercalation of VOF_3 and fluorine was pointed out. The electrochemical insertion of lithium into $C_{17.7}(VOF_3)F$ was investigated by chronopotentiometry and a.c. impedance spectroscopy in propylene carbonate–1 M $LiClO_4$. The chemical diffusion coefficient, $\tilde{D}_{Li}$, was estimated to be close to 4.0×10^{-10} cm^2 s^{-1} for all the values of the intercalation ratio of lithium under study ($0 < y < 1.5$).

Keywords: Lithium intercalation; Graphite intercalation compounds; Lithium batteries

1. Introduction

Since several years, graphite fluoride (denoted CF_x) has been proposed as a cathodic material in primary lithium batteries with an organic electrolyte containing a lithium salt. Such kinds of batteries are commercially available. These generators are based on the intercalation of lithium cations in the host structure. They exhibit some advantages with respect to Zn/MnO_2 batteries: the e.m.f. (about 3 V) and the energy density are two times and five times higher, respectively and the discharge curve is very flat. Nevertheless, their performances are limited notably because of the non-reversibility of the electrochemical intercalation of Li^+ into the host structure and the very low electrical conductivity. The latter strongly depends on the x values. For example, the electrical conductivity of $CF_{0.192}$ and $CF_{0.515}$ are equal to 125 and 5×10^{-8} S cm^{-1}, respectively [1]. In order to avoid these problems, graphite intercalation compounds (GICs) have been proposed recently [2,3] as an alternative of graphite fluoride as the positive material in primary lithium batteries. These compounds can be obtained at low temperature (< 150 °C) in the presence of a suitable catalyst (HF, MgF_2, etc.) and show, in most cases, higher electrical conductivity than the initial graphite. For example, Nakajima and Touma [4] have shown that the electrical conductivity of C_xF (with $x \leq 0.3$), prepared from HOPG in the presence of fluorine and HF, is about 5×10^4 S cm^{-1}, and only 10^4 S cm^{-1} for the initial graphite. Other kinds of GICs can be prepared using volatile transition metal oxide fluoride. Oxidative atmosphere is needed for the intercalation of volatile transition metal oxide fluoride into graphite [5–7]. For example, Touzain et al. [5] have synthesized GICs with VOF_3 under high chlorine pressure (from 10 to 20 atm) in the 20–90°C temperature range. Vasse et al. [6] have prepared a $C_{40}VOF_3$–GIC in anhydrous liquid HF. $C_x(VOF_3)F$ vanadium oxide fluoride GICs were synthesized recently by Nakajima et al. [8] using fluorine and V_2O_5. The electrical conductivity of such compounds is very high and close to 10^6 S cm^{-1}.

The aim of this paper is to present the preparation method, the structural features (deduced from X-ray photoelectron spectroscopy (XPS) and X-ray diffraction (XRD)) and the electrochemical behaviour (using chronopotentiometry and a.c. impedance measurements) of these $C_x(VOF_3)F$ compounds prepared from V_2O_5 and graphite in a fluorine atmosphere.

* Corresponding author.

PII S0378-7753(96)02410-X

2. Experimental

2.1. Preparation of $C_x(VOF_3)F$ with $x = 17.2$ to 38.8

Natural graphite powder (57–74 μm) was used for the preparation of the graphite intercalation compounds. Two nickel vessels containing natural graphite powder and V_2O_5 powder were put in a vertical nickel reactor. The temperature of the reactor was gradually increased up to 130 °C under high vacuum and then high purity fluorine gas supplied by Daikin Industries, Ltd. (purity F_2: 99.4–99.7%, N_2: 0.3–0.6% and HF < 0.01%) was introduced at 1 atm. The temperature and the pressure were maintained during 24 h. The fluorination of V_2O_5 gives rise mainly to gaseous VOF_3 which is intercalated together with fluorine into the host graphite. The obtained compounds were denoted $C_x(VOF_3)F$ with $x = 17.2$–38.8.

2.2. Analysis of the products

The structural analysis of $C_x(VOF_3)F$ samples was made from XRD patterns obtained with a Shimadzu XD-610 X-ray diffractometer with a Cu Kα radiation and a nickel filter. The chemical interaction between carbon, fluorine, vanadium and oxygen was estimated by XPS analysis using a ULVAC-PHI model 5500 spectrometer with a Mg Kα excitation source. The calibration of the spectrometer was made at binding energies 75.1 and 932.6 eV for $Cu3p_{3/2}$ and $Cu2p_{3/2}$, respectively.

2.3. Electrochemical measurements

The electrochemical measurements were performed in 1 M $LiClO_4$–propylene carbonate (PC) at 25 °C using a glass beaker cell in a dry box under argon atmosphere [9,10]. A conducting agent (graphite) was added to the electroactive $C_x(VOF_3)F$ compound (weight ratio 1:1). The cathodic pellet (diameter: 13 mm) was prepared by compression-moulding this mixture onto a nickel mesh under a pressure of 180 kg cm^{-2}, and subsequent drying during one day at 80 °C. The thickness of the pellet was about 0.4 mm and the mass of the electroactive compound was about 5 mg. The pellet was then put between two glass fiber porous separators in order to avoid dispersion of the powder in the electrolyte. Lithium pellets were used both as counter and reference electrodes. The counter-electrodes were arranged in front of both sides of the working electrode.

Discharge curves were obtained with a Tohogiken Potentiostat 2000. A.c. impedance measurements were carried out by coupling the potentiostat with a NF Electronics Instruments S-5720B frequency response analyser. The frequency range was 10^5–10^{-3} Hz and the amplitude of the sinusoidal signal was 5 mV peak-to-peak. The quasi-equilibrium open-circuit voltage (OCV) was measured after 24 h on open circuit, when the potential shift was stabilised to less than 0.2 mV h^{-1}.

Table 1
X-ray diffraction data for $C_x(VOF_3)F$ compounds. Number of graphite sheets between two successive layers of intercalated species (stage); repeat distance along the c-axis (I_c)

Sample	Stage	I_c (Å)
$C_{17.2}(VOF_3)F$	2	11.39
$C_{17.7}(VOF_3)F$	2	11.34
$C_{20.2}(VOF_3)F$	2	11.34
$C_{20.4}(VOF_3)F$	2	11.38
$C_{21.1}(VOF_3)F$	2	11.22
$C_{29.7}(VOF_3)F$	2 + 3 or 4	11.26
$C_{38.8}(VOF_3)F$	2 + high	11.21

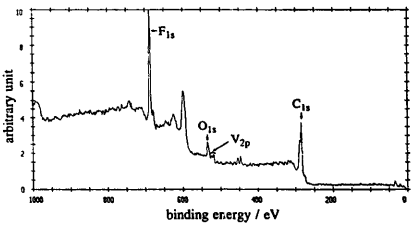

Fig. 1. XPS survey spectrum of $C_{20.4}(VOF_3)F$.

3. Results and discussion

3.1. Structural characterisation of $C_x(VOF_3)F$ samples

XRD measurements were performed with vanadium oxide fluoride–graphite intercalation compounds. The stage number, defined as the number of graphite sheets between two successive layers of intercalated species, was deduced from the repeat distance along the c-axis (I_c value), calculated from the (001) diffraction lines. The composition, the stage number and the I_c values are given in Table 1. The size of vanadium oxide fluoride intercalate, d_i, can be calculated from I_c values. The experimental determination of d_i leads to an average value, i.e. 4.6 Å, which was found to be independent of the composition and the stage number. This value is in a good agreement with the value obtained from geometric considerations (4.7 Å) [8].

XPS is a suitable tool for studying the elemental composition of a sample through the analysis of electron core level peaks [11,12]. It also provides information about the oxidation state of the elements, deduced from the chemical shifts in binding energies [12–15]. The survey spectrum of $C_{20.4}(VOF_3)F$, shown in Fig. 1, displays the photoelectron peaks of C_{1s}, F_{1s}, O_{1s} and V_{2p} electrons. Identical observations were made with all other samples. Each peak was decomposed into several contributions. Individual fitting parameters used for each region (binding energy (BE) and full width at half-maximum peak height (FWHM)) are given in Table 2. For each sample, the V_{2p} region is composed of two sym-

Table 2
Results of XPS investigations on $C_x(VOF_3)F$ compounds; fitting parameters: binding energy (eV), full width at half-maximum peak height (eV)

Sample	C_{1s}			O_{1s}			F_{1s}			$V2p_{3/2}$			$V2p_{1/2}$		
	BE (eV)	FWHM (eV)	Chemical bond	BE (eV)	FWHM (eV)	Chemical bond	BE (eV)	FWHM (eV)	Chemical bond	BE (eV)	FWHM (eV)	Chemical bond	BE (eV)	FWHM (eV)	Chemical bond
$C_{17.2}(VOF_3)F$	283.4	1.5	C–C	529.5	1.9	V=O	682.6	2.0	V–F	516.0	1.5	V=O	523.1	1.5	V=O
	285.0	2.6	$(C–O)_a$	531.2	2.4	$(C–O)_a$	684.9	2.4	C–F[1]	516.9	2.2	V–F	524.3	2.2	V–F
	288.1	2.4	C–F	533.5	2.5	$(C–O)_b$	686.9	2.5	C–F[2]						
	290.8	2.9	$(C–O)_b$												
$C_{17.7}(VOF_3)F$	283.3	1.4	C–C	529.3	1.8	V=O	682.4	1.6	V–F	515.9	1.8	V=O	522.9	1.8	V=O
	285.0	2.5	$(C–O)_a$	530.8	2.0	$(C–O)_a$	684.1	1.6	C–F[1]	517.3	2.3	V–F	524.5	2.3	V–F
	288.1	2.0	C–F	532.2	2.5	$(C–O)_b$	686.8	2.4	C–F[2]						
	290.5	2.4	$(C–O)_b$												
$C_{20.2}(VOF_3)F$	283.5	1.5	C–C	529.3	1.7	V=O	682.5	1.7	V–F	515.9	1.4	V=O	522.9	1.4	V=O
	285.0	2.3	$(C–O)_a$	530.7	2.3	$(C–O)_a$	685.0	1.5	C–F[1]	516.9	2.2	V–F	524.2	2.2	V–F
	288.1	2.4	C–F	533.2	2.6	$(C–O)_b$	686.8	2.4	C–F[2]						
	290.9	2.6	$(C–O)_b$												
$C_{20.4}(VOF_3)F$	283.5	1.4	C–C	529.5	1.7	V=O	682.6	1.8	V–F	516.0	1.4	V=O	523.0	1.4	V=O
	284.7	2.8	$(C–O)_a$	531.1	2.3	$(C–O)_a$	684.5	2.3	C–F[1]	516.9	2.2	V–F	524.4	2.2	V–F
	288.3	2.4	C–F	533.9	2.6	$(C–O)_b$	687.0	2.7	C–F[2]						
	291.1	2.6	$(C–O)_b$												
$C_{21.1}(VOF_3)F$	283.6	1.7	C–C	529.8	1.9	V=O	683.1	2.1	V–F	515.7	1.5	V=O	522.1	1.5	V=O
	285.0	2.9	$(C–O)_a$	532.1	2.2	$(C–O)_a$	685.2	1.9	C–F[1]	517.3	2.2	V–F	523.8	2.2	V–F
	288.1	2.6	C–F	533.9	2.3	$(C–O)_b$	687.0	2.2	C–F[2]						
	290.9	2.0	$(C–O)_b$												
$C_{29.7}(VOF_3)F$	283.6	1.4	C–C	529.2	1.7	V=O	682.7	1.9	V–F	516.0	1.5	V=O	523.0	1.5	V=O
	285.3	2.8	$(C–O)_a$	530.7	2.5	$(C–O)_a$	684.2	1.5	C–F[1]	516.7	2.2	V–F	524.3	2.2	V–F
	288.0	2.5	C–F	533.2	2.6	$(C–O)_b$	686.7	2.5	C–F[2]						
	290.9	2.5	$(C–O)_b$												
$C_{38.8}(VOF_3)F$	283.7	1.5	C–C	529.3	1.7	V=O	682.7	1.8	V–F	516.0	1.4	V=O	523.1	1.4	V=O
	285.5	2.7	$(C–O)_a$	530.8	2.2	$(C–O)_a$	684.5	2.9	C–F[1]	516.9	2.3	V–F	524.4	2.3	V–F
	288.1	2.5	C–F	533.3	2.6	$(C–O)_b$	686.9	2.4	C–F[2]						
	290.8	2.7	$(C–O)_b$												

[1] Nearly ionic bond.
[2] Semi-ionic bond.

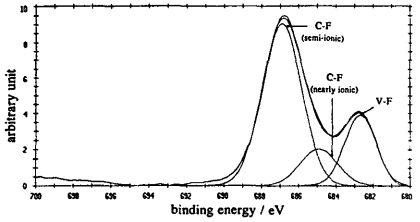

Fig. 2. XPS analysis of $C_{17.1}(VOF_3)F$; high resolution spectrum of F_{1s} region.

metrical doublet peaks situated at 515.8 ± 0.2, 523.0 ± 0.1, 517.0 ± 0.3, and 524.1 ± 0.4 eV. It clearly shows the co-existence of V–F and V=O bonds [8], respectively. The peak intensity ratio of V–F to V=O contributions is approximately 3 corresponding to the F:O atomic ratio in VOF_3. Whatever the composition of the $C_x(VOF_3)F$ samples, the O_{1s} region is composed of three peaks: the peak at lower binding energy (BE = 529.5 ± 0.3 eV) is assigned to V=O bonds. The two other peaks at higher energy (531.4 ± 0.7 and 533.0 ± 0.8 eV) may be attributed to two kinds of C–O bonds [16–19]. The latter C–O bonds were also observed in the C_{1s} region. The presence of such kinds of C–O bonds suggests the existence of some excess oxygen in the graphite gallery and in the contaminated layer at the surface of the sample. As it was reported previously [8], the co-intercalation of a small amount of VO_2F_2 might occur. The excesses of oxygen are probably generated from the decomposition of co-intercalated VO_2F_2 because it is less stable than VOF_3. The F_{1s} region is composed of three peaks at BE = 682.7 ± 0.4 eV, BE = 684.6 ± 0.6 eV and BE = 686.8 ± 0.2 eV which are assigned to V–F bond, nearly ionic C–F bond and semi-ionic C–F bond, respectively. For example, the F_{1s} region for $C_{17.1}(VOF_3)F$ is presented in Fig. 2.

All these analyses have shown that VOF_3 and fluorine were intercalated into the host material and that some excess of oxygens were also present.

3.2. Electrochemical properties of $C_{17.7}(VOF_3)F$ samples

The electrochemical insertion of lithium cations into $C_{17.7}(VOF_3)F$ was studied. The discharge and recharge curves obtained with a current intensity $I = 0.14$ mA in PC–$LiClO_4$ 1 M at 25 °C is presented in Fig. 3. The cycles were carried out in the potential range 1.2–4.4 V versus Li/Li^+. Whatever the number of cycles, a gradual decrease in discharge potential and a gradual increase in recharge potential, respectively were observed, without any plateau, versus the lithium intercalation ratio, y. Such a behaviour is characteristic of a multiphase electrode material. After 20 cycles, 90–100% of the discharge capacities were recovered during the recharge step. Therefore, cycles can be performed with this kind of electrode material without apparent modification of the structure with time. On the contrary, it is well known that

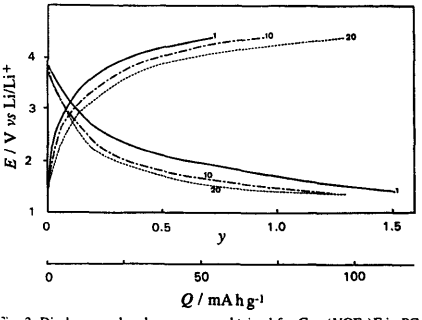

Fig. 3. Discharge and recharge curves obtained for $C_{17.7}(VOF_3)F$ in PC–$LiClO_4$ 1 M at 25 °C vs. lithium intercalation ratio, y, or recharge/discharge capacity, Q (mAh g^{-1}). Discharge current intensity: 0.14 mA. The curves correspond to the 1st, 10th and 20th cycles.

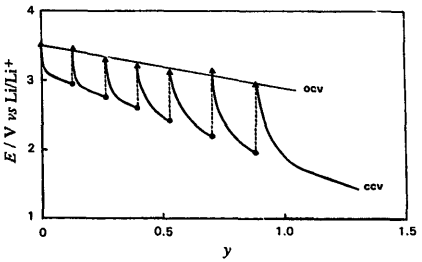

Fig. 4. Equilibrium open-circuit potential: (▲) experimental data, and (———) simulated curve and closed-circuit voltage of $C_{17.7}(VOF_3)F$ in PC–$LiClO_4$ 1 M at 25 °C vs. lithium intercalation ratio, y. Discharge current intensity: 0.14 mA.

the discharge of graphite fluoride gives rise to a high and flat plateau which corresponds to the formation of a conducting compound, Li_xCF_x. The latter is decomposed further into LiF and carbon; this fact explains the non reversibility of the electrochemical intercalation of lithium into CF_x.

The kinetic characteristics of lithium insertion into $C_{17.7}(VOF_3)F$ can also be obtained from impedance measurements. First, a galvanostatic pulse was applied to the electrode during a sufficient time for reaching one value of y. Second, the current was interrupted and the electrode tended gradually towards equilibrium. It corresponds to one equilibrium potential, called OCV, as it is shown in Fig. 4, because of the slow diffusion of lithium from the surface to the bulk of the host material. Finally, impedance measurement was performed at that equilibrium potential corresponding to one value of y. After the impedance measurement, another galvanostatic pulse was applied to the electrode, etc.

Typical a.c. impedance responses for several values of the intercalation ratio, $y = 0.27, 0.40$ and 0.76, are given in Fig. 5. Whatever the y values, this response can be described by the

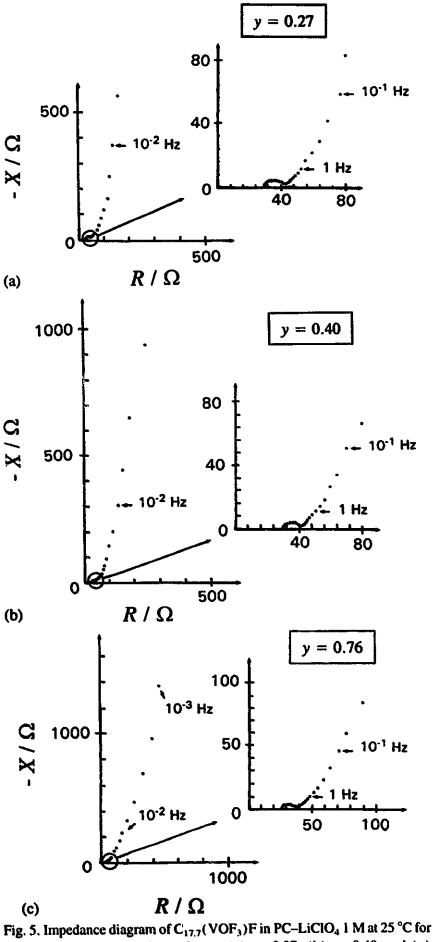

Fig. 5. Impedance diagram of $C_{17,7}(VOF_3)F$ in PC–$LiClO_4$ 1 M at 25 °C for several lithium intercalation ratios, y: (a) $y=0.27$; (b) $y=0.40$, and (c) $y=0.76$.

Randles equivalent circuit [20] comprising R_e, the ohmic drop in the electrolyte, R_{ct}, the charge-transfer resistance of the reaction, C_{dl}, the double-layer capacitance, and Z_W, the Warburg impedance.

As it was difficult to determine the electroactive surface area, the kinetic parameters deduced from the impedance measurements will be referred to the apparent surface area, S, which is assumed to be equal to $S_0 \times 0.5$ (where S_0 is the geometric surface area of the pellet) in order to take into account the weight ratio between the electroactive compound and graphite (1:1).

At high frequency, the semi-circle in the Nyquist diagram is related to the charge-transfer phenomenon. At low frequency, a straight line showing a 45° angle on the real axis is obtained. It corresponds to the Warburg impedance [20] (semi-infinite diffusion). A second straight line showing a higher slope is observed at lower frequencies due to the finite thickness of the electrode which induces a finite length diffusion process. For ideal cases, the slope of this branch is infinite. Ho et al. [20] have shown that the chemical lithium diffusion coefficient, $\tilde{D}_{Li}$, may be obtained by solving Fick's law with appropriate initial and boundary conditions. These authors have shown that the Warburg impedance has a constant-phase angle of 45° and is expressed as

$$Z_W = A_\omega (1-j)\omega^{-1/2} \quad (1)$$

where ω is the angular frequency of the signal. The coefficient A_ω is given by:

$$A_\omega = \frac{V_M(dE/dy)}{\sqrt{2}nF\tilde{D}_{Li}^{1/2}S} \quad (2)$$

where V_M, is the molar volume of the host structure, dE/dy, the slope of the OCV versus y values, n the number of exchanged electrons during the electrochemical reaction, F the Faraday constant, and S the apparent surface area.

Eq. (2) is valid only if the semi-infinite diffusion conditions are fulfilled ($\omega \gg 2\tilde{D}_{Li}/L^2$ where L is the finite length). Thus, the chemical diffusion coefficient, $\tilde{D}_{Li}$, may be obtained from the expression of A_ω.

The slope of the linear plot $|Z_W| - \omega^{-1/2}$ leads to the determination of $\tilde{D}_{Li}$. The phase difference, φ, between the current and the voltage is independent of frequency and is theoretically equal to 45° but experimental values $\varphi = 45° \pm 5°$ are found. Moreover, the high frequency semi-circle is flattened. These two phenomena are probably due to the microscopic surface roughness of the electrode as discussed by de Levie [21]. The $\tilde{D}_{Li}$ values for $C_{17,7}(VOF_3)F$ are roughly the same, for all the Li^+ concentration range: 4.0×10^{-10} cm^2 s^{-1} and in the same order of magnitude as those obtained with another powdered host material such as $Li_yV_2O_5$ (with $y=0$ to 1) [22].

As discussed by Weppner and Huggins [23], the chemical diffusion coefficient is related to the component diffusion coefficient, D_{Li}, by the following equation

$$\tilde{D}_{Li} = D_{Li}\frac{d\ln(a_{Li})}{d\ln(c_{Li})} = -D_{Li}\frac{F}{RT}\frac{dE}{dy} \quad (3)$$

where $[d\ln(a_{Li})]/[d\ln(c_{Li})]$ is the thermodynamic enhancement factor, which is calculated from the slope dE/dy of the OCV curve versus y for the $C_x(VOF_3)F$ compound. The activity, a_{Li}, and the concentration, c_{Li}, are referred to neutral lithium. An exponential decrease of D_{Li} from 9.5×10^{-11} to 1.7×10^{-11} cm^2 s^{-1} with increasing y

values ($y=0.13$–0.88) is observed due to the decreasing probability to find an unoccupied site close to an occupied one.

The exploitation of the high-frequency semi-circle of the Nyquist diagrams leads to the determination of the charge-transfer resistance, at equilibrium potential, for a given intercalation ratio. The exchange current density, J_0, is related to R_{ct} by

$$J_0=\frac{RT}{nFSR_{ct}} \quad (4)$$

It is found that, for this sample, J_0 is constant within the y range: 1.2×10^{-3} A cm^{-2} as in the case of V_2O_5 [22] or WO_3 [24]. Such a behaviour may suggest that the interfacial charge-transfer process is associated with Li^+ ion transfer between the electrolyte and the host material. Nevertheless, this value is about 50 times higher than that obtained with V_2O_5 by Farcy et al. [22]. It means that the interfacial charge transfer reaction is faster with $C_x(VOF_3)F$.

4. Conclusions

The structural and the electrochemical properties of $C_x(VOF_3)F$ (with $17.2\leq x\leq 38.8$) graphite intercalation compounds were studied. XRD measurements have shown that the stage number of the prepared compounds was almost the same and equal to 2. Co-intercalation of fluorine and VOF_3 occur simultaneously during the preparation step. Ionic and semi-ionic C–F bonds were pointed out by XPS analysis.

Contrary to graphite fluorides for which the discharge reaction is irreversible, discharge/recharge cycles can be performed with these compounds without apparent modification of the host structure. The chemical coefficient diffusion and the exchange current density, obtained from impedance measurements, were close to 4×10^{-10} cm^2 s^{-1} and 1×10^{-3} A cm^{-2}, respectively.

Acknowledgements

The authors wish to thank Mrs Nobuko Kumagai and Dr Y. Matsuo for their assistance in the experimental work.

References

[1] T. Mallouk and N. Bartlett, *J. Chem. Soc., Chem. Commun.*, (1983) 103.
[2] N. Watanabe, T. Nakajima and H. Touhara, *Graphite Fluorides*, Elsevier, Amsterdam, 1988, Ch. 8, p. 240.
[3] T. Nakajima and N. Watanabe, *Graphite Fluorides and Carbon–Fluorine Compounds*, CRC Press, Boca Raton, FL, 1991, Ch. 6, p. 142.
[4] T. Nakajima and M. Touma, *J. Fluorine Chem.*, *57* (1992) 83.
[5] P. Touzain, E. Buscarlet and L. Bonnetain, *Rev. Chim. Miner.*, *14* (1977) 482.
[6] R. Vasse, G. Furdin, J. Melin and A. Herold, *Carbon*, *19* (1981) 249.
[7] A. Hamwi, P. Touzain and L. Bonnetain, *Rev. Chim. Miner.*, *19* (1982) 651.
[8] T. Nakajima, Y. Nagai and M. Motoyama, *Eur. J. Solid State Inorg. Chem.*, *29* (1992) 919.
[9] N. Kumagai, S. Tanifuji and K. Tanno, *J. Power Sources*, *35* (1991) 313.
[10] N. Kumagai, S. Tanifuji, F. Fujiwara and K. Tanno, *Electrochim. Acta*, *37* (1992) 1039.
[11] N.H. Turner, *Analytical Instrumentation Handbook*, Galen Wood Ewing, New York, 1990, Ch. 15.
[12] D. Briggs and J.C. Rivière, in D. Briggs and M.P. Seah (eds.), *Practical Surface Analysis*, Wiley, New York, 1983, p. 113.
[13] K. Siegbahn, *Ann. Phys.*, *3* (1968) 281.
[14] D. Briggs, *Handbook of X-Ray and Ultraviolet Photoelectron Spectroscopy*, Heyden and Son, London, 1971.
[15] C.D. Wagner, W.M. Riggs, L.E. Davis, J.F. Moulder and G.E. Mullenberg, in G.E. Mullenberg (ed.), *Handbook of X-Ray Photoelectron Spectroscopy*, Perkin-Elmer Corporation, Eden Prairie, MN, 1979.
[16] L. Bai and B.E. Conway, *J. Appl. Electrochim.*, *20* (1990) 916.
[17] H. Groult, D. Devilliers, M. Vogler, C. Hinnen, P. Marcus and F. Nicolas, *Electrochim. Acta*, *38* (1993) 2413.
[18] R.L. McCreery, *Electroanal. Chem.*, *17* (1991) 221.
[19] C. Kozlowski and P.M.A. Sherwood, *J. Chem. Soc.*, *81* (1985) 2745.
[20] C. Ho, I.D. Raistrick and R.A. Huggins, *J. Electrochem. Soc.*, *127* (1980) 343.
[21] R. de Levie, *Adv. Electrochem. Electrochem. Eng.*, *6* (1967) 329.
[22] J. Farcy, R. Messina and J. Perichon, *J. Electrochem. Soc.*, *137* (1990) 1337.
[23] W. Weppner and R.A. Huggins, *Rev.. Mater. Sci.*, *8* (1978) 269.
[24] I.D. Raistrick, *Solid State Ionics*, *9–10* (1983) 425.